Clock Steering Using Frequency Estimates from Stand-alone GPS Receiver Carrier Phase Observations

Edward Byrne[1], Thao Q. Nguyen [2], Lars Boehnke [1] , Frank van Graas[3], and Samuel Stein [1]

[1]Symmetricom Corporation, 4775 Walnut Street Suite 1B, Boulder, USA
[2]AFRL/RYMN, 2241 Avionics Circle, WPAFB, USA
[3]Ohio University, 231 Stocker Center, Athens, USA
ebyrne@symmetricom.com

Abstract—Carrier phase observations from a stand-alone GPS receiver are used to estimate the frequency of a clock for the purpose of steering it to GPS System Time. Utilization of this frequency estimate can significantly improve the frequency stability performance of a class of timing systems where an oven controlled crystal oscillator is disciplined by GPS time difference estimates. In these systems, the frequency difference estimates are more stable than both the local oscillator and the GPS clock time difference estimates over intermediate time intervals. Oscillator disciplining using these frequency difference estimates enables improved mid-term frequency stability without incurring the size, weight, and power costs of an atomic frequency reference.

Key words: GPS Carrier Phase, Clock Steering, Frequency Estimation

I. INTRODUCTION

Coherent combination of data from a network of distributed sensors requires time and frequency synchronization across the sensor network. This paper focuses on improving the performance of a class of timing systems where cost and size, weight, and power (SWaP) considerations limit the options for improving frequency stability performance.

Time and frequency reference systems typically employ a layered approach to achieve desired phase noise and frequency stability performance over a range of time intervals. The final output stage is chosen to meet the phase noise and short-term frequency stability requirements of the application. If longer-term frequency stability is required, the output stage oscillator is typically steered to one or more clocks that have the desired frequency stabilities over progressively longer time intervals. In GPS disciplined timing systems, time difference measurements between the local clock and GPS System Time made by the GPS receiver are typically used in the final steering stage, with the longest time constant.

The GPS receiver clock time difference estimates come from the code phase solution for position and time. These time difference estimates are too noisy over short time intervals for use in disciplining high performance quartz crystal oscillators with a short time constant control loop. Depending on the performance of the quartz oscillator, the GPS clock time difference estimates are typically averaged over tens to hundreds of seconds before they are stable enough to be of use in disciplining the quartz oscillator.

In systems where cost and SWaP allow it, the quartz crystal oscillator is often steered to an atomic frequency reference (e.g. Rubidium) at an intermediate time constant, and the timing system is steered to GPS clock time difference measurements at a longer time constant. Addition of the atomic frequency

standard offers significant improvement in frequency stability over intermediate time intervals, where the quartz crystal's performance is inadequate and the GPS clock time difference estimates are too noisy to be of help. Systems that cannot bear the cost or SWaP of an atomic oscillator often discipline the output stage oscillator directly with GPS time difference estimates. At intermediate time intervals, the frequency stability performance is limited by the better of the oscillator frequency stability and the GPS clock time difference estimate stability.

This paper focuses on the class of timing systems consisting of an oven controlled crystal oscillator (OCXO) and a GPS receiver. We use an algorithm that generates a clock frequency difference estimate from GPS carrier phase observations, and apply those estimates to the problem of steering the local clock to GPS System Time.

II. GPS CARRIER PHASE PROCESSING ALGORITHM

Reference [1] describes an algorithm that uses carrier phase observations from a stand-alone GPS receiver to generate precise estimates of platform velocity and the frequency difference between the GPS receiver clock and GPS system time. This algorithm uses single differences (SD) in time of carrier phase observations for each GPS space vehicle (SV) to estimate the average velocity and average clock frequency difference over the time interval between the two sets of carrier phase observations. Referencing Figure 1, the algorithm uses carrier phase observations at times t_1 and t_2 to estimate the change in receiver antenna position, $\Delta\boldsymbol{b}$, and the change in receiver clock offset, $\Delta\delta t_{rcvr}$, over the time interval $[t_1,t_{t2}]$. The $\Delta\boldsymbol{b}$ and $\Delta\delta t_{rcvr}$ quantities are converted to average velocity and average clock frequency difference, respectively, by dividing by the time interval t_2-t_1.

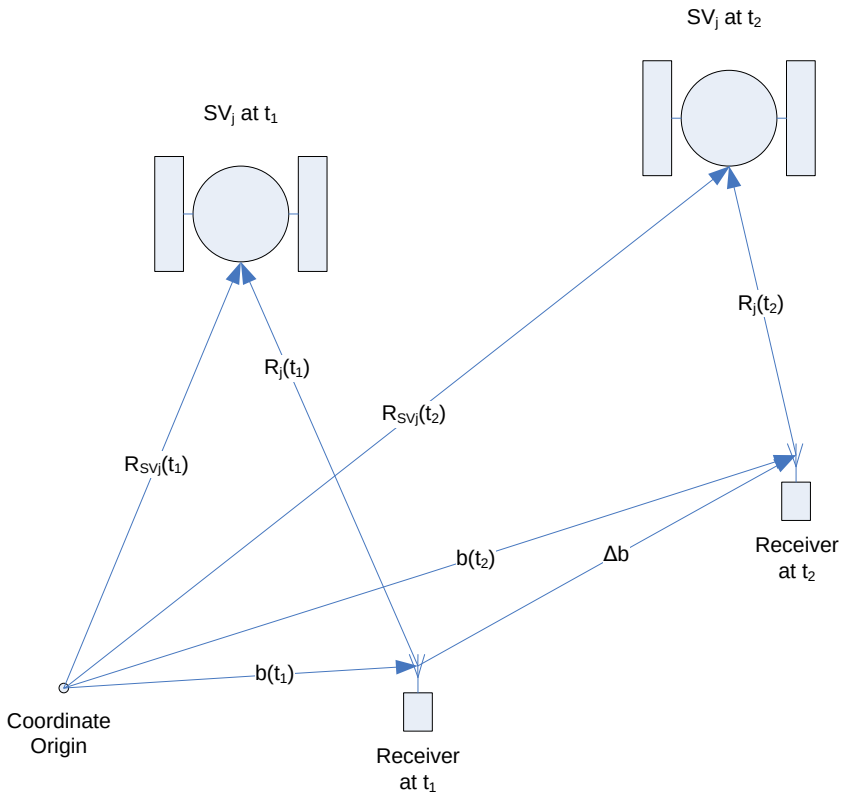

Figure 1. Receiver / Single SV Geometries Across Two Observation Epochs.

The processing starts with the raw single difference in time of carrier phase range measurements (i.e. accumulated Doppler range) for each SV_j:

$$\Delta\varphi_j = \varphi_j(t_2) - \varphi_j(t_1) \tag{1}$$

Each $\Delta\boldsymbol{\varphi}_j$ from equation (1) is adjusted and compensated as follows:

- Compensate for the change in SV clock bias from t_1 to t_2 (SV clock model from broadcast ephemeris);
- Compensate for the change in ionospheric delay from t_1 to t_2 (accomplished by using combined L1 and L2 carrier phase range for $\varphi_j(t)$);
- Adjust for SV Doppler;
- Adjust for the receiver/satellite geometry change from t_1 to t_2.

After the above described compensations and adjustments, the single difference in time of carrier phase ranges for SV_j is called $\Delta\varphi_j^{comp\ \&\ adj}$. This quantity, combined with the geometry from Figure 1, relates known quantities to the unknowns $\Delta\boldsymbol{b}$ and $\Delta\delta t_{rcvr}$. The vectors of interest are:

- $\boldsymbol{R}_{SVj}(t)$ Position of SV_j at time t (from broadcast ephemeris)
- $\boldsymbol{b}(t)$ Receiver antenna position at time t (from code range single point position solution)

$\boldsymbol{e}_j(t)$ is the unit vector from the receiver antenna to the j^{th} SV, SV_j

$$\boldsymbol{e}_j(t) = \frac{\boldsymbol{R}_{SVj}(t) - \boldsymbol{b}(t)}{|\boldsymbol{R}_{SVj}(t) - \boldsymbol{b}(t)|} \tag{2}$$

Equation (3) gives the relationship between the known quantities for SV_j and the unknowns $\Delta\boldsymbol{b}$ and $\Delta\delta t_{rcvr}$. The < , > notation indicates a vector inner product operation.

$$\Delta\varphi_j^{comp\ \&\ adj} = < -\mathbf{e}_j(t_2), \Delta\mathbf{b} > + \Delta\delta t_{rcvr} \tag{3}$$

With observations from N or more SV's ($N \geq 4$), one can define a system of equations, one for each SV, that relates the carrier phase observations and other known quantities to the unknowns $\Delta\boldsymbol{b}$ and $\Delta\delta t_{rcvr}$.

$$H\,\boldsymbol{x} = \boldsymbol{y} \tag{4}$$

$$H = \begin{bmatrix} -\boldsymbol{e}_1^T(t_2) & 1 \\ -\boldsymbol{e}_2^T(t_2) & 1 \\ \cdots & \cdots \\ -\boldsymbol{e}_N^T(t_2) & 1 \end{bmatrix} \tag{5}$$

$$\boldsymbol{x} = \begin{bmatrix} \Delta\widehat{\boldsymbol{b}} \\ \Delta\widehat{\delta t}_{\boldsymbol{rcvr}} \end{bmatrix} \tag{6}$$

$$\boldsymbol{y} = \begin{bmatrix} \Delta\hat{\varphi}_1^{comp\ \&\ adj} \\ \Delta\hat{\varphi}_2^{comp\ \&\ adj} \\ \cdots \\ \Delta\hat{\varphi}_N^{comp\ \&\ adj} \end{bmatrix} \tag{7}$$

We use the pseudo inverse method to calculate the least squares estimates of $\Delta\boldsymbol{b}$ and $\Delta\delta t_{rcvr}$.

$$\hat{\boldsymbol{x}} = (H^{\boldsymbol{T}}H)^{-\mathbf{1}}H^{\boldsymbol{T}}\boldsymbol{y} \tag{8}$$

Finally, the clock frequency difference estimate is calculated as the change in receiver clock offset over the measurement interval.

$$\hat{f}_{rcvr} = \frac{\Delta\hat{\delta}t_{rcvr}}{t_2 - t_1} \tag{9}$$

This processing algorithm has several characteristics that make it suitable for real time frequency estimation in tactical environments as well as other applications. Since the algorithm only uses GPS receiver measurements from two subsequent measurement epochs, the algorithm starts up quickly and recovers quickly from disruptions in GPS measurement data. The residuals from the least squares solution provide a ready check on the quality of the solution. These residuals are useful for both the identification of problem SV's (e.g. multi-path, low C/N_0) and the characterization of the quality of the overall solution (e.g. based on a composite look at all SV residuals).

III. CHARACTERIZATION OF THE CLOCK FREQUENCY DIFFERENCE ESTIMATE

We characterized the noise floor of the clock frequency difference estimates by conducting an experiment where the accuracy and stability of the GPS receiver's frequency reference input is below the noise floor of the clock frequency difference estimate. In this configuration, any variation in the clock frequency difference estimate is attributable to the measurement noise of the frequency difference estimates. Figure 2 shows the test setup. The GPS receiver, a NovAtel OEMV1, is a dual frequency receiver capable of receiving an external frequency reference. The external frequency reference is driven by our house timing system.

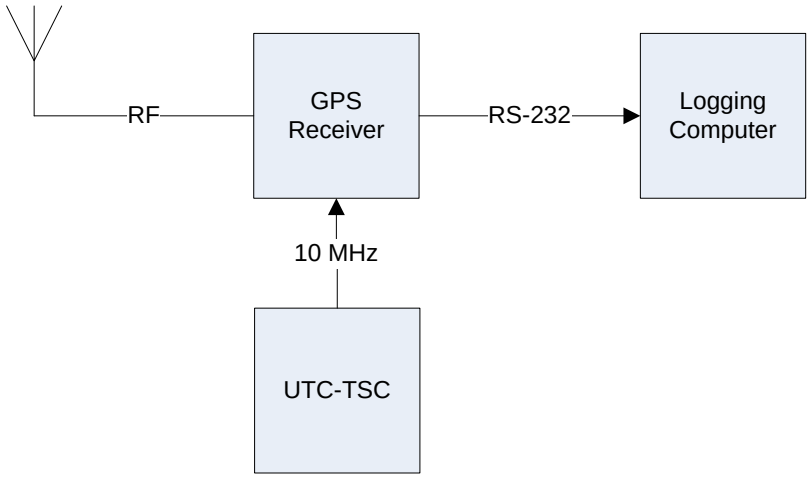

Figure 2. Test Setup For Characterization of Clock Frequency Difference Estimate Noise Floor.

We collected the RANGECMPA (@2 Hz), CLOCKMODELA (@ 2 Hz), and RAWEPHEMA logs from the OEMV1 GPS receiver and processed the data as follows:

Run the carrier phase processing algorithm to generate a time series of clock frequency difference estimates. Calculate the Allan deviation of the clock frequency difference estimates.

Parse the CLOCKMODELA message to get the GPS receiver's clock time difference estimate (the instantaneous range bias field in the CLOCKMODELA message). Calculate the Allan deviation of the clock time difference estimates.

Figure 3 shows the frequency stabilities of the clock frequency difference estimates from carrier phase processing, the clock time difference estimates from the GPS receiver's code phase solution, and an undisciplined OCXO. Note that the carrier phase processing's clock frequency difference estimate is

significantly more stable than the clock time difference estimate for time intervals less than several thousand seconds.

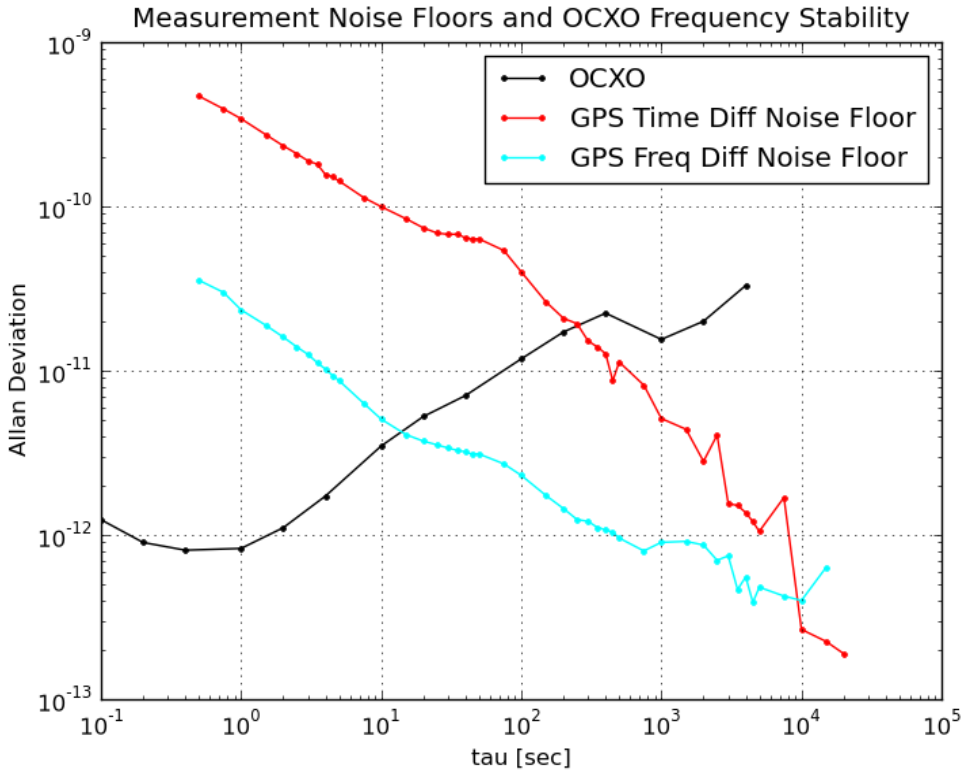

Figure 3. Measurement Noise Floors Compared to OCXO Frequency Stability.

IV. APPLICATION TO CLOCK STEERING

Referring to Figure 3, a well designed timing system using the GPS clock time difference measurements to steer the OCXO would achieve the frequency stability of the OCXO for short time intervals, and the frequency stability of the GPS clock time difference measurements for longer time intervals. The transition from OCXO to GPS would occur approximately at the time interval of the intersection of the respective Allan deviations.

With the new clock frequency difference estimate available, a well designed system should achieve the frequency stability of the OCXO for short time intervals, the stability of the GPS clock frequency difference estimates for intermediate time intervals, and the stability of GPS clock time difference estimates for long time intervals. Again the transitions occur at time intervals approximately at the intersections of the Allan deviations.

To achieve the desired composite frequency stability, we incorporated the clock frequency difference estimate into our Kalman clock state estimator. The Kalman filter models the oscillator with three states (phase, frequency, and aging) as shown in Figure 4. Our prior implementation of this Kalman filter ingests GPS clock time difference estimates only, providing direct observation of only the phase state. For this work, we modified the Kalman filter implementation to absorb both GPS clock time difference estimates and GPS clock frequency difference estimates, providing direct observations of two of the three states of the clock model.

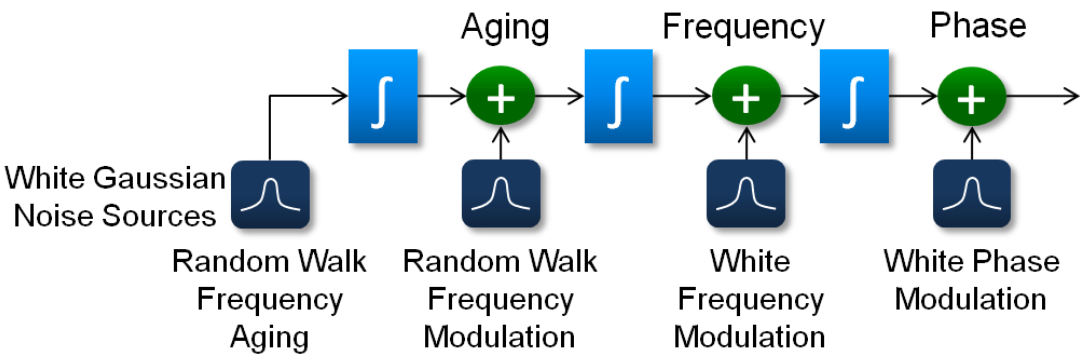

Figure 4. Three State Clock Model Used by Kalman Filter.

Figure 5 shows the test setup used to explore the application of the carrier phase processing clock frequency difference estimate to the steering of an OCXO to GPS System Time. The GPS receiver is the same unit as in Figure 2. Now the GPS receiver's external frequency reference comes from an OCXO that can be steered by the clock estimation and control subsystem. The clock estimation and control subsystem is implemented in software, and can be configured to use different estimators (ranging from a Kalman filter to no estimator) and clock control algorithms (e.g. state variable feedback). Now, the carrier phase processing subsystem executes in real time on an embedded computer; it receives raw observations and ephemeris data from the GPS receiver and generates the clock frequency difference estimate using the method described in Section II. The stability of the OCXO is measured against the house timing system using a Symmetricom 5120 Phase Noise Test Set.

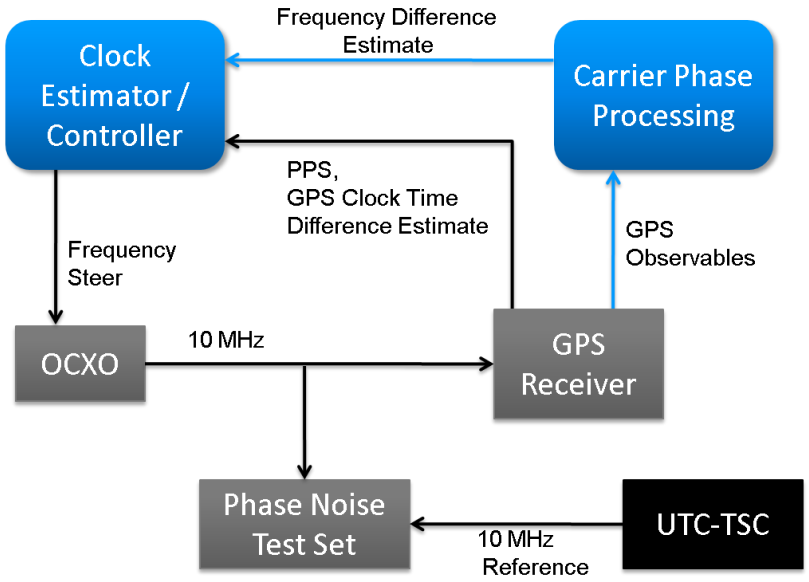

Figure 5. Closed Loop Clock Steering Test Setup.

Figure 6 and Figure 7 show the clock steering performance using the Kalman filter modified to absorb the clock frequency difference estimates. The Symmetricom 5120 Phase Noise Test Set is used to compare the OCXO's behavior to the house timing system. Clock time and frequency difference measurements are calculated from the phase noise test set's raw phase measurement data using a 1 second integration period to smooth the data. The time domain plots show the improved performance as indicated by decreased

medium term phase variation and decreased frequency wander. Since the long time interval behavior is determined by the GPS clock time difference estimates, and those estimates are common to both implementations, the long term phase deviation of both systems are the same. However, as Figure 8 shows, we do expect a significant (~2.5X) decrease in the peak to peak frequency drift of the steered clock based on the difference between the local maxima of Allan deviations.

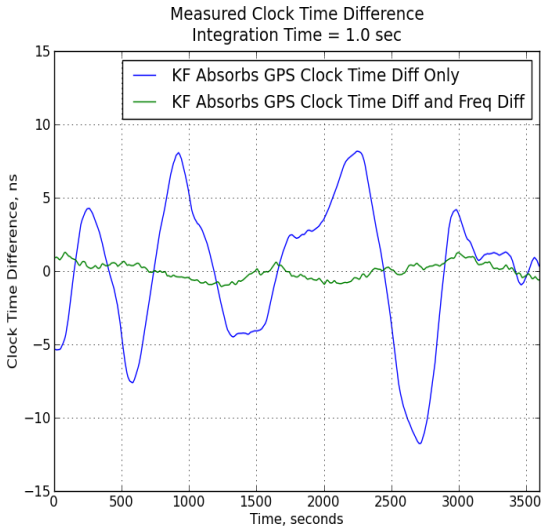

Figure 6. Measured Clock Time Difference Modified Kalman Filter.

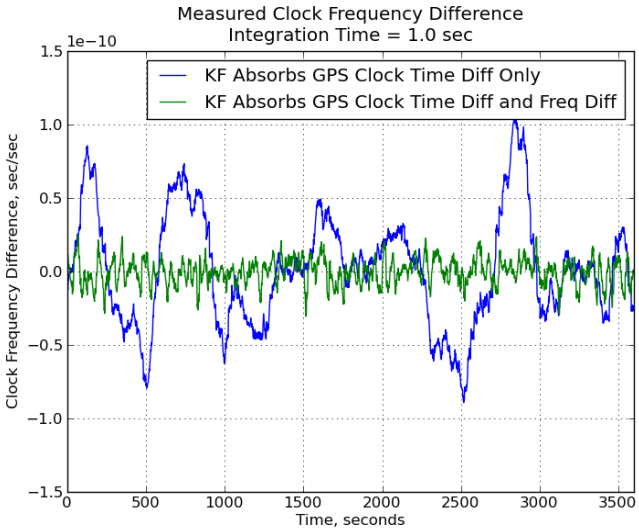

Figure 7. Measured Clock Frequency Difference Modified Kalman Filter.

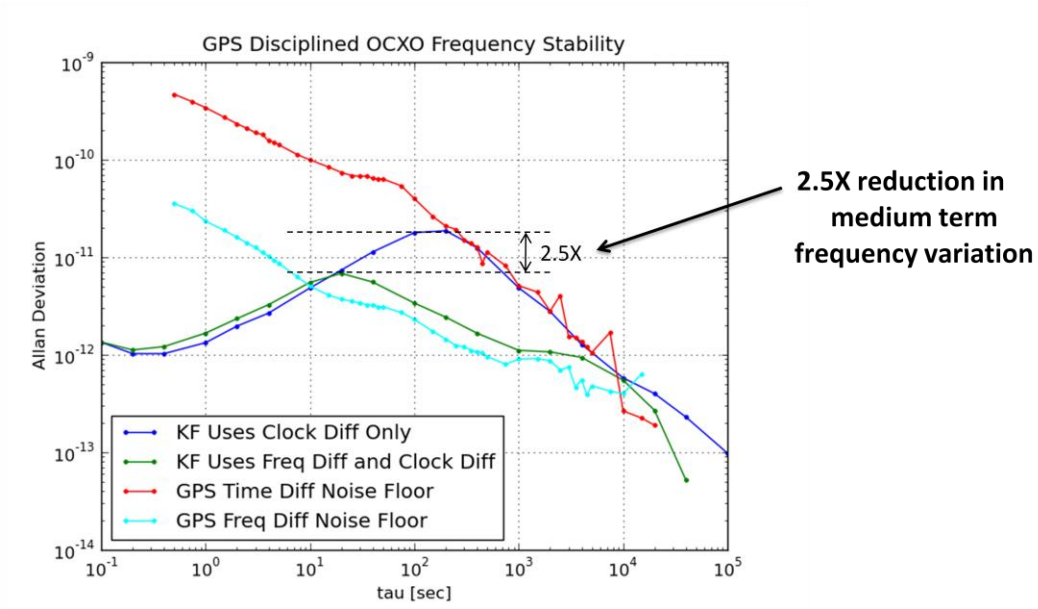

Figure 8. Closed Loop Frequency Stability Comparison: Original versus Modified Kalman Filter.

Frequency references on Intelligence, Surveillance, and Reconnaissance (ISR) sensor platforms are exposed to changes in temperature, acceleration, and magnetic field that can introduce significant frequency transients. Here we explore the detection and suppression of these transients with the measurements available from a GPS receiver. Consider the case where a frequency reference experiences a 1e-11 shift in frequency caused by platform dynamics. Figure 9 shows that it takes approximately 100

times longer to detect the frequency transient with GPS clock time difference measurements than it does with the GPS clock frequency difference measurements.

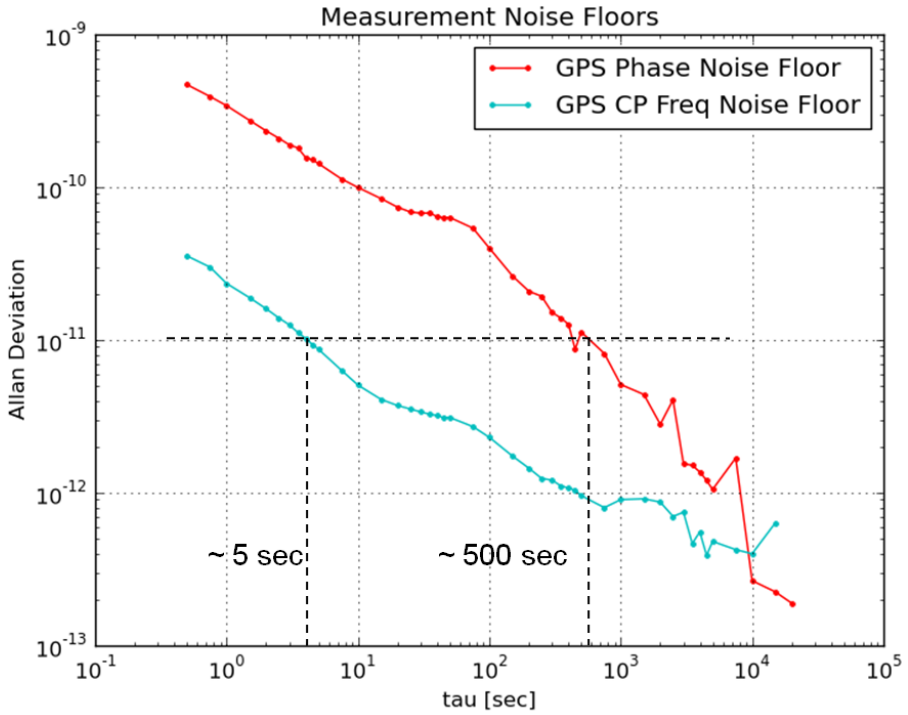

Figure 9. Frequency Transients Observable In Less Time With Frequency Difference Estimate Compared To Clock Difference Estimate.

In order to use the clock frequency difference estimate to improve the transient response of the timing system, we need to move away from the Kalman filter using the state model shown in Figure 4. Since that approach does not model the relatively large and rapid frequency changes associated with changes in acceleration, the Kalman filter will show undesirable behavior when absorbing measurements associated with such a transient. Perhaps the simplest approach to deal with this challenge is to discard the Kalman filter altogether and use a simple Frequency Lock Loop (FLL) to steer the OCXO based on clock frequency difference estimates. We tested the FLL implementation by executing "tip tests", changing the OCXO orientation in the static gravitational field in order to emulate acceleration changes caused by flight dynamics. The FLL absorbs a new frequency estimate every 4 seconds, and the control loop has a 10 second time constant. Figure 10 shows the efficacy of the FLL approach in improving the transient response compared to a Kalman filter that absorbs only clock time difference estimates.

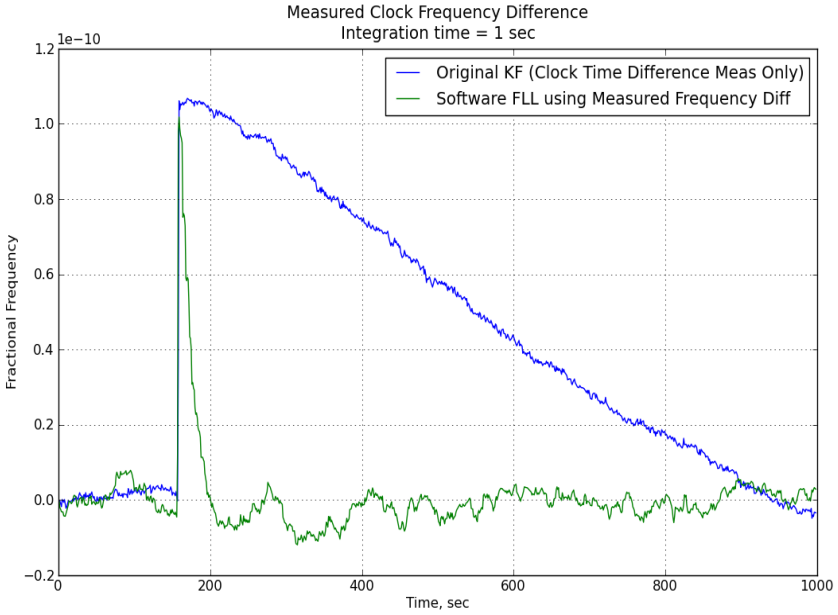

Figure 10. FLL Using Clock Frequency Difference Estimates Improves Transient Response.

V. CONCLUSIONS

We explored characteristics and applications of an algorithm that uses carrier phase measurements from a stand-alone GPS receiver to generate precise velocity and clock frequency difference estimates. We found the clock frequency difference estimates to have desirable frequency stability properties, supporting their use in clock frequency estimation and control applications. We found that the clock frequency difference estimates were more stable over intermediate time intervals than both an OXCO and the GPS clock time difference estimates from a GPS receiver. For timing systems that are limited to a GPS receiver and an OCXO, incorporation of these clock frequency difference estimates enables a significant reduction in the frequency wander of the steered clock. This reduction in drift is very important to a network of distributed sensors and timing systems as it provides a one-for-one reduction in the range of frequency variation across sensor nodes. The clock frequency difference estimates are also useful for frequency transient detection, enabling more rapid detection of transients than is possible with GPS clock time difference estimates.

ACKNOWLEDGMENT

This work was performed under the Multi-INT Reference Optimization for Distributed Sensing (MIRODS) program, funded by the AFRL Sensors Directorate at Wright Patterson Air Force Base.

REFERENCES

[1] F. van Graas and A. Soloviev, "Precise velocity estimation using a stand-alone GPS receiver," NAVIGATION: Journal of the Institute of Navigation, Vol. 51, No. 4, pp. 283-292, 2004.